Crack Initiation Angles in Functionally Graded Materials under Mixed Mode Loading

Alpay Oral [a], Jorge L. Abanto-Bueno [b], John Lambros [c], Gunay Anlas [a]

[a] *Department of Mechanical Engineering, Bogazici University, Bebek, Istanbul, TURKEY*
[b] *Department of Mechanical Engineering, Bradley University, Peoria, IL 61625, USA*
[c] *Department of Aerospace Engineering, University of Illinois at Urbana-Champaign, Urbana, IL 61801, USA*

Abstract. In this study, quasi-static crack initiation under mixed mode loading in planar (2-D) functionally graded materials is presented. First, crack initiation in the homogeneous material which forms the basis of our FGM – polyethylene – is studied. The Generalized Maximum Tangential Stress Criterion (GMTS) is applied through use of finite elements to determine crack initiation angles in a cracked 2-D functionally graded material. The effects of crack length, T-stress, inherent length scale r_c and mode mixity are discussed. Computational results of crack initiation angles are compared to experimental results obtained using functionally graded polyethylene. Stress Intensity factors for a center cracked FGM are calculated.

Keywords: FGM, Crack initiation angle, Mixed mode fracture, Digital image correlation

K_I, K_{II}, *T*-STRESS AND CRACK INITIATION ANGLES FOR AN EDGE CRACKED GEOMETRY UNDER MIXED-MODE LOADING

The crack tip displacement field is obtained experimentally using Digital Image Correlation (DIC) method, and numerically, using the FE method. Stress intensity factors K_I, K_{II} and the *T*-stress are evaluated applying a least squares minimization to the near crack-tip displacement field. Crack initiation angles are determined by calculating the maximum $\sigma_{\theta\theta}$ [1, 2] value around the crack tip for different r_c/a values, where a is the crack length and r_c is inherent length scale for application of the criterion. The use of r_c is dictated by the generalized Maximum Tensile Stress criterion which states that when the hoop stress reaches a critical value at a certain distance r_c away from the tip, then failure occurs. For the case of homogeneous materials r_c has been obtained through parametric FEA studies that are matched to experimental data. In the present work we extend this approach, of using the generalized MTS criterion and matching r_c to experiments, to crack initiation angles of FGMs. First, homogeneous materials are studied to check the validity of each method for two specimens; then, three different functionally graded plates are studied.

Homogeneous Material

As homogeneous material, 50 hours UV (ultraviolet) irradiated, 0.406 mm thick ECO (poly-ethylene carbon monoxide) sheet is used. Its elastic properties are:

CP973, *Multiscale and Functionally Graded Materials 2006*
edited by G. H. Paulino, M.-J. Pindera, R. H. Dodds, Jr., F. A. Rochinha, E. V. Dave, and L. Chen

$$E = 280MPa, \qquad \nu = 0.45. \tag{1}$$

In Fig. 1, an edge cracked specimen geometry and applied load is shown. Two specimens with $\pi/3$ and $\pi/6$ crack inclination angles, ϕ, respectively, are studied (Table 1).

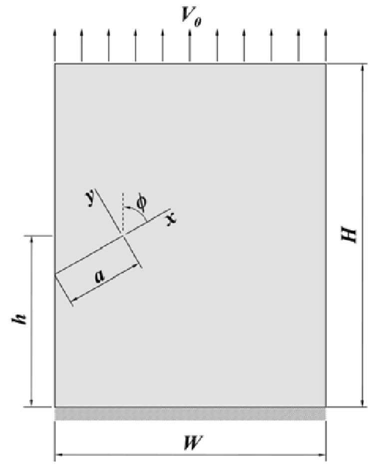

FIGURE 1. Edge cracked specimen, V_0 is the applied displacement.

TABLE 1. Dimensions of edge cracked specimens

	H (mm)	*W* (mm)	*h* (mm)	*a* (mm)
Specimen-$\pi/3$	90	70	45	33
Specimen-$\pi/6$	90	70	45	40

The displacement field is obtained experimentally using DIC for both specimens. The displacement field along y-direction asymptotically near the crack-tip is:

$$u_y = \underbrace{\frac{K_I}{2\mu_{tip}}\left(\frac{r}{2\pi}\right)^{\frac{1}{2}}\sin\frac{\theta}{2}\left(\frac{3-\nu_{tip}}{1+\nu_{tip}}-\cos\theta\right)-\frac{T\nu_{tip}}{2\mu_{tip}(1+\nu_{tip})}r\sin\theta}_{\text{Mode I loading}} \\ \underbrace{+\frac{K_{II}}{4\mu_{tip}}\left(\frac{r}{2\pi}\right)^{\frac{1}{2}}\left(\frac{5\nu_{tip}-3}{1+\nu_{tip}}\cos\frac{\theta}{2}-\cos\frac{3\theta}{2}\right)}_{\text{Mode II loading}}\underbrace{+A_1 r\cos\theta+u_{0y}}_{\text{R.B.}} \tag{2}$$

Least squares minimization is applied to the displacement field u_y near the crack-tip (Eq. 2) at crack initiation to determine K_I, K_{II} and T-stress. A similar procedure is followed using finite elements and K_I, K_{II} and T-stress are evaluated for both specimens. The results are tabulated in Table 2.

TABLE 2. Experimental and numerical results of K_I, K_{II} and T-stress values for the homogeneous edge cracked specimens

	ϕ	K_I (MPam$^{0.5}$)	K_{II} (MPam$^{0.5}$)	T (MPa)
Exp. results	$\pi/3$	0.903	0.245	-0.784
	$\pi/6$	0.745	0.526	5.536
Num. results	$\pi/3$	0.851	0.304	-0.753
	$\pi/6$	0.747	0.566	5.272

Crack initiation angles, α, are measured experimentally and also predicted using max $\sigma_{\theta\theta}$ values obtained through FE analysis for different r_c/a values (Table 3). Agreement between the two is reasonably good.

TABLE 3. Crack initiation angles for the homogeneous edge cracked specimens

	Crack initiation angles, α (°)		
	Experimental	**FE Result (Max $\sigma_{\theta\theta}$)**	
Specimen-π/3		-32.4	for r_c/a=0.01
	-28±1.5	-31.3	for r_c/a=0.05
		-30.8	for r_c/a=0.1
Specimen-π/6		-52.5	for r_c/a=0.01
	-52±1.5	-54.3	for r_c/a=0.05
		-54.5	for r_c/a=0.1

Functionally Graded Material

Three different loading and material property gradient orientations are studied.
Case I: Material property gradient is perpendicular to the crack.
Case II: There is an inclination between material property gradient and the crack.
Case III: Material property gradient is parallel to the crack but loading is not.

Poisson's ratio, ν, is 0.45 and Young's Moduli, E, are given explicitly on Figs. 2, 3 and 4. The FGMs are manufactured by selective ultraviolet irradiation poly(ethylene carbon monoxide)—a photo-sensitive copolymer that becomes more brittle and stiffer under ultraviolet irradiation [3]. Specimen geometries, loadings and material property variations are given in Fig. 2-4 for Cases I-III, respectively.

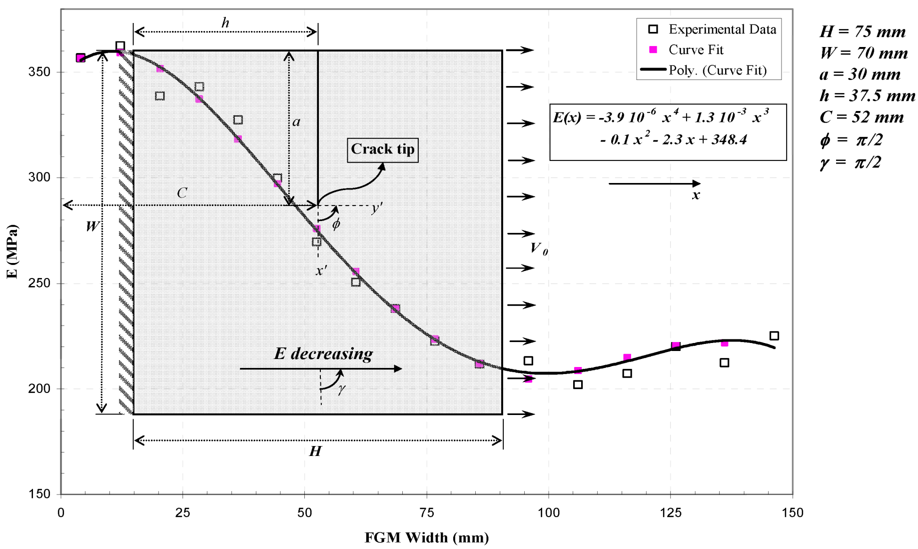

FIGURE 2. Geometry, loading and material property for Case I - FGM.

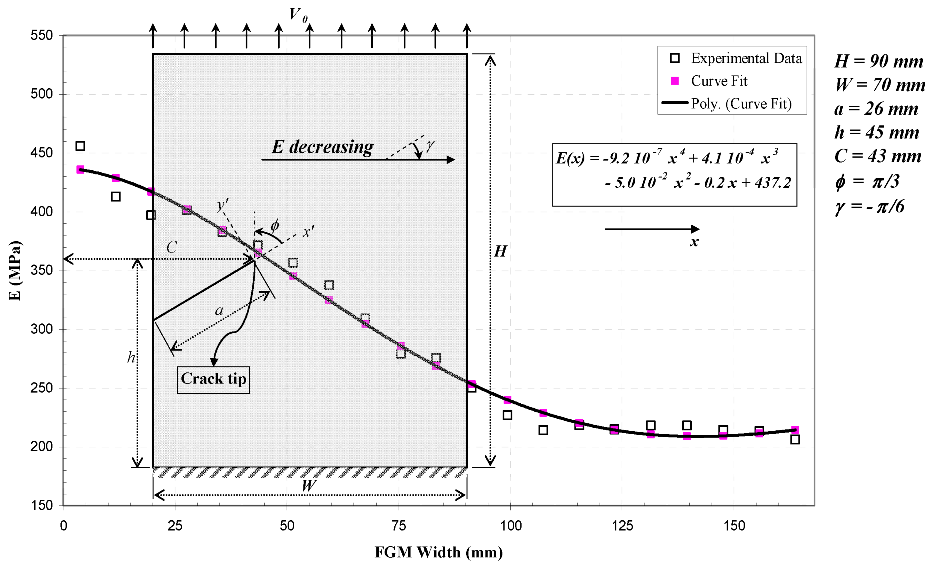

FIGURE 3. Geometry, loading and material property for Case II - FGM.

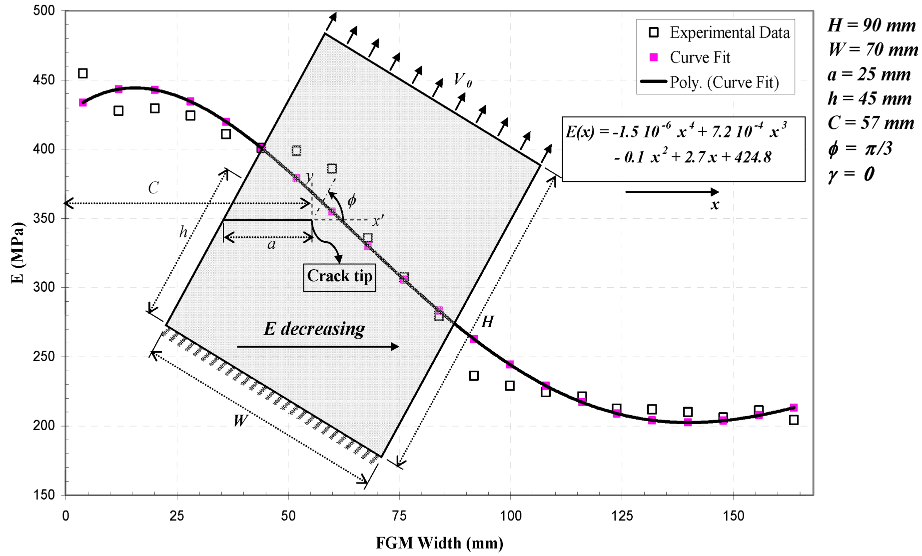

FIGURE 4. Geometry, loading and material property for Case III - FGM.

K_I, K_{II} and *T*-stress are obtained using the same procedure used for homogenous materials. These values are tabulated in Table 4 for each case analyzed. Experimentally measured and numerically predicted crack initiation angles are given in Table 5. With the exception of Case III, where the curve fit to elastic modulus, E, data is off especially around the crack tip, agreement between the two is good. In Case III, experimental and numerical results deviate.

TABLE 4. Experimental and numerical results of K_I, K_{II} and *T*-stress values for the FGM edge cracked specimens

	Case	K_I ($MPam^{0.5}$)	K_{II} ($MPam^{0.5}$)	*T* (MPa)
Exp. results	*I*	0.554	0.039	-4.272
	II	0.755	0.179	-0.063
	III	0.969	0.224	-0.930
Num. results	*I*	0.534	0.058	-2.860
	II	0.714	0.169	-0.902
	III	0.868	0.232	-1.127

TABLE 5. Crack initiation angles for the FGM edge cracked specimens

	Crack initiation angles, α (°)		
	Experimental	**FE Result (Max $\sigma_{\theta\theta}$)**	
Case I		-1.4	for r_c/a=0.01
	0	-0.6	for r_c/a=0.05
		-0.1	for r_c/a=0.1
Case II		-31.4	for r_c/a=0.01
	-28±1.5	-30.1	for r_c/a=0.05
		-29.8	for r_c/a=0.1
Case III		-30.3	for r_c/a=0.01
	-19±1.5	-29.3	for r_c/a=0.05
		-29.3	for r_c/a=0.1

In Tables 2 and 4, K_I, K_{II} and T-stresses are calculated using asymptotic displacement equation, Eq. 2, and are sensitive to the size of K-dominant region. Results obtained can improve if a different region around the crack tip is used

NUMERICAL STRESS INTENSITY FACTOR CALCULATIONS

Mixed-mode stress intensity factors are calculated using J(0) as described by Anlas, *et al.* [4] and mode extraction technique [5] for a center cracked specimen (See Fig. 5). Results are compared to the results of Konda & Erdogan [6] and Kim & Paulino [7] and tabulated in Table 6.

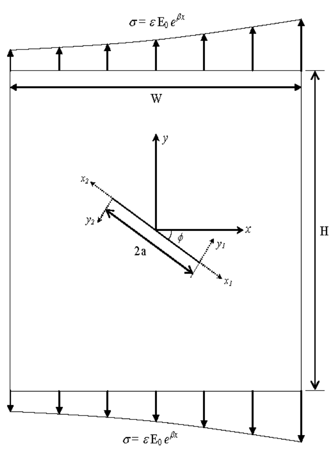

FIGURE 5. Center cracked FGM plate.

TABLE 6. Normalized stress intensity factors for $\beta a = 0.25$ and $\beta a = 0.50$

Method		$\beta a = 0.25$				$\beta a = 0.50$			
	ϕ/π	$k_I(a)$	$k_{II}(a)$	$k_I(-a)$	$k_{II}(-a)$	$k_I(a)$	$k_{II}(a)$	$k_I(-a)$	$k_{II}(-a)$
Present	0	1.209	0	0.830	0	1.448	0	0.680	0
study	0.1	1.087	-0.319	0.760	-0.258	1.303	-0.340	0.628	-0.217
	0.2	0.780	-0.526	0.554	-0.419	0.927	-0.559	0.479	-0.365
	0.3	0.404	-0.513	0.297	-0.437	0.474	-0.535	0.251	-0.395
Konda and	0	1.196	0	0.825	0	1.424	0	0.674	0
Erdogan [7]	0.1	1.081	-0.321	0.750	-0.254	1.285	-0.344	0.617	-0.213
	0.2	0.781	-0.514	0.548	-0.422	0.925	-0.548	0.460	-0.365
	0.3	0.414	-0.504	0.290	-0.437	0.490	-0.532	0.247	-0.397
Kim and	0	1.221	0	0.827	0	1.458	0	0.664	0
Paulino	0.1	1.101	-0.325	0.752	-0.250	1.310	-0.353	0.608	-0.207
(MMC) [7]	0.2	0.789	-0.519	0.549	-0.416	0.933	-0.558	0.454	-0.355
	0.3	0.414	-0.507	0.291	-0.432	0.487	-0.536	0.244	-0.386
Kim and	0	1.220	0	0.840	0	1.446	0	0.679	0
Paulino (J^*_k-	0.1	1.106	-0.315	0.769	-0.239	1.306	-0.341	0.628	-0.195
integral) [7]	0.2	0.810	-0.494	0.582	-0.390	0.944	-0.534	0.488	-0.329
	0.3	0.404	-0.523	0.297	-0.439	0.461	-0.563	0.256	-0.392
Kim and	0	1.235	0	0.854	0	1.461	0	0.693	0
Paulino	0.1	1.140	-0.312	0.775	-0.248	1.315	-0.333	0.633	-0.209
(DCT) [7]	0.2	0.802	-0.499	0.565	-0.412	0.943	-0.529	0.469	-0.356
	0.3	0.423	-0.489	0.297	-0.425	0.498	-0.512	0.249	-0.384

CONCLUSIONS

For the use of asymptotic equations, the knowledge of K-dominant region is important as shown in Tables 2 and 4. Numerical mixed mode stress intensity factors obtained using J(0) and mode extraction method [4, 5] are in good agreement with the analytical results (Table 6).

ACKNOWLEDGMENTS

This study was supported by National Science Foundation (NSF) through grant NSF-INT-0322271. Gunay Anlas and Alpay Oral acknowledge partial support of the State Planning Agency (DPT) through grant DPT 01 K 120270.

REFERENCES

1. F. Erdogan and G. C. Sih, *J. Basic Eng.-Trans ASME* **85**, 519-525 (1963).
2. J. G. Williams and P. D. Ewing, *Int. J. Frac. Mech.* **8**, 441-446 (1972).
3. J. Abanto-Bueno and J. Lambros, *Exp. Mech.* **46**, 179-196 (2006).
4. G. Anlas, M. H. Santare, J. Lambros, *Int. J. Frac.* **104**, 131-143 (2000).
5. C. Mattheck and H. Moldenhauer, *Int. J. Frac.* **34**, 209-218 (1987).
6. N. Konda and F. Erdogan, *Eng. Fract. Mech.* **47**, 533-545 (1994).
7. J. H. Kim and G. H. Paulino, *Int. J. Numer. Meth. Engng.* **53**, 1903-1935 (2002).